Geophysical Research Letters

RESEARCH LETTER
10.1029/2025GL115983

Large and Increasing Biospheric Productivity of Northern Ecosystems

Matthias Cuntz[1], Benjamin Smith[2,3], Josep G. Canadell[4], Jürgen Knauer[2,4,5], and Vanessa Haverd[4†]

[1]Université de Lorraine, AgroParisTech, INRAE, UMR Silva, Nancy, France, [2]Hawkesbury Institute for the Environment, Western Sydney University, Penrith, NSW, Australia, [3]Department of Physical Geography and Ecosystem Science, Lund University, Lund, Sweden, [4]CSIRO Environment, Canberra, ACT, Australia, [5]School of Life Sciences, Faculty of Science, University of Technology Sydney, Ultimo, NSW, Australia

[†]Deceased January 2021.

Key Points:

- The amplitude of the seasonal cycle of CO_2 provides a constraint to changing land biosphere productivity in the northern hemisphere
- Plant productivity and its increase need to be larger than most estimates to explain the increase in the CO_2 seasonal cycle amplitude
- The increase in amplitude is primarily driven by productivity, while carbon release has a counteracting effect, reducing the amplitude

Supporting Information:

Supporting Information may be found in the online version of this article.

Correspondence to:

M. Cuntz,
matthias.cuntz@inrae.fr

Citation:

Cuntz, M., Smith, B., Canadell, J. G., Knauer, J., & Haverd, V. (2025). Large and increasing biospheric productivity of northern ecosystems. *Geophysical Research Letters*, *52*, e2025GL115983. https://doi.org/10.1029/2025GL115983

Received 15 MAR 2025
Accepted 28 JUN 2025

Author Contributions:

Conceptualization: Matthias Cuntz, Vanessa Haverd
Data curation: Matthias Cuntz
Formal analysis: Matthias Cuntz, Vanessa Haverd
Funding acquisition: Matthias Cuntz, Josep G. Canadell, Vanessa Haverd
Investigation: Matthias Cuntz, Benjamin Smith, Jürgen Knauer, Vanessa Haverd
Methodology: Matthias Cuntz, Benjamin Smith, Vanessa Haverd
Software: Matthias Cuntz
Supervision: Josep G. Canadell
Validation: Matthias Cuntz
Visualization: Matthias Cuntz

Abstract Plants take up carbon dioxide (CO_2) through photosynthesis. How this will change with rising CO_2 concentrations in the atmosphere will strongly determine future climate change. An increase in the seasonal variations of atmospheric CO_2 in recent decades indicates a positive trend in photosynthetic carbon uptake. We combined data-driven seasonal cycles of plant productivity with carbon sinks across the range predicted by current biospheric process models to explain the seasonal variations of CO_2 at high and low northern latitudes over the past 40 years. We find that increases in seasonal variations can only be explained by a larger gross primary productivity (GPP) of northern ecosystems than most current estimates and by an increase of GPP about proportional to the increase in atmospheric CO_2, also larger than most current estimates. Our results provide an improved constraint to estimate the future behavior of the terrestrial carbon sink.

Plain Language Summary How much carbon are land ecosystems taking up annually, and how will this uptake change with climate change and rising CO_2 levels? We give new insights into these critical questions by analyzing data on the atmospheric concentration of CO_2. The latter varies due to seasonal changes in plant photosynthesis with this seasonal variation becoming larger in recent decades. By disentangling the contributing processes to these changes using data-driven estimates together with global vegetation models, we demonstrate that northern ecosystems must exhibit high productivity and a substantial increase in productivity with rising CO_2, both values exceeding most current estimates.

1. Introduction

Carbon dioxide (CO_2) concentrations in the atmosphere vary seasonally, reflecting changes in the balance between growing season uptake of CO_2 through photosynthesis of the terrestrial biosphere and the release of CO_2 throughout the year by plant and soil respiration (Bacastow et al., 1985; Forkel et al., 2016; Keeling et al., 1996). The amplitude of this seasonal cycle (ASC) is increasing with time, and doing so at a faster rate in high northern latitudes compared to lower latitudes (Bacastow et al., 1985; Graven et al., 2013; Keeling et al., 1996). This has been interpreted as an indication that plant productivity is increasing faster in high northern ecosystems than in temperate and tropical ecosystems (Forkel et al., 2016; Graven et al., 2013; Keeling et al., 1996).

A large body of literature has examined the increase in ASC (Bacastow et al., 1985; Forkel et al., 2016; Gray et al., 2014; Keeling et al., 1996; Lin et al., 2020; Liu et al., 2024; Piao et al., 2017; Randerson et al., 1997, 1999; Thomas et al., 2016; Zeng et al., 2014) as well as special features of ASC time series, such as the temporary slowdown of the increase at Mauna Loa, Hawaii (MLO, 20°N), from 1985 to 2010 (Buermann et al., 2007; Piao et al., 2008; Wang et al., 2020; Zhu et al., 2018). The studies agree that there is a larger increase in plant productivity in high northern ecosystems (Graven et al., 2013; Randerson et al., 1999), mediated by warming-induced increases in growing season length (Keeling et al., 1996; Piao et al., 2008). Increases in plant productivity could also result from CO_2 fertilization of photosynthesis under increasing atmospheric CO_2 (Ito et al., 2016; Piao et al., 2017), from warming of the land surface (Forkel et al., 2016; Piao et al., 2017), and from associated increases in vegetation cover and density, visible from space as vegetation greening (Forkel et al., 2016; Ito et al., 2016). In addition, the intensification of agriculture with higher crop yields and multiple cropping in the second half of the 20th century might have contributed to the observed increase in ASC (Gray et al., 2014; Zeng et al., 2014), but the effects are likely small, particularly in high northern latitudes (Chen et al., 2019; Forkel et al., 2016; Wang et al., 2020).

Writing – original draft: Matthias Cuntz
Writing – review & editing: Benjamin Smith, Josep G. Canadell, Jürgen Knauer

The literature is less consistent about the role of respiration in the increase of ASC. Increases at MLO before the 1990s were attributed in part to enhanced respiration in Europe (Keeling et al., 1996) due to hotter autumn temperatures (Piao et al., 2008, 2017), but increases in the early 2000s could not be explained by respiration changes (Barichivich et al., 2013; Buermann et al., 2007; Wang et al., 2020). Hence, the relative contributions of the uptake (photosynthesis) and release (respiration) flux components behind the ASC increase remain unclear. No study has been able to explain simultaneously the zonal differences in the amplitudes of the seasonal cycle and their temporal increases, that is, simultaneously explaining the absolute values and the temporal increases of ASC at both the mid-latitudes and the high northern latitudes. Reconciling the different mechanisms involved in the observed dynamics in the two regions would provide fundamental information to assess future changes in vegetation productivity under anthropogenic climate change.

Forkel et al. (2016) successfully simulated the absolute values and temporal increase of ASC at high northern latitudes with a biospheric process model, but they showed a rather large offset of ASC relative to atmospheric observations at the mid-latitudes. Thomas et al. (2016) and Haverd et al. (2020) showed that no model among the suite of current biospheric process models was able to reproduce either the absolute value or the temporal increase of ASC. The latter authors were able to tune the output respiration fluxes of one of the models (CABLE-POP) so that the resulting atmospheric CO_2 reproduced the absolute value and the trend at high northern latitudes. This was accomplished by artificially moving the respiration fluxes in time such that the modeled net flux had the correct seasonal timing. Here we build further on these contributions and show that we can reconcile absolute values and temporal increases of ASC at mid and high northern latitudes by imposing productivity and the correct seasonal variations of land surface carbon fluxes of northern ecosystems.

2. Materials and Methods

We combined data-driven estimates of the Seasonal Cycles (SC) of photosynthesis (namely gross primary productivity (GPP)) and net ecosystem exchange (NEE, Jung et al., 2011) with annual sink strengths from biospheric process models (Le Quéré et al., 2018; Sitch et al., 2015). This gave a full factorial experiment of the three factors: plant productivity, its increase with time, and the size and spatial pattern of the net land carbon sink for the last 40 years. In general, data-driven estimates show much better SC than model estimates (Peng et al., 2015), while models show more realistic carbon sinks because they take a more complete set of processes into account (Jung et al., 2020). We hence combined the strengths of these approaches by using the seasonal variations of GPP and NEE from Jung et al. (2011) for 2006–2008 to calculate seasonal variations of respiration (RESP) that together yield a very good timing of the SC of atmospheric CO_2 (Peng et al., 2015). By taking only the seasonal variations (subtracting the annual mean NEE, cf. Text S1 in Supporting Information S1), these fields had initially zero annual sinks or sources at each grid cell. The data-driven estimates give a global GPP of about 120 PgC a^{-1} around 2007 (Beer et al., 2010), but the actual number is uncertain. Here we use the data-driven global flux maps of Jung et al. (2011), which were scrutinized in many analyses in the literature. Other data-driven estimates sometimes give larger plant productivity in high northern latitudes (Nelson et al., 2024) while other give smaller plant productivities there (Virkkala et al., 2021). We hence tried plausible scenarios of plant productivity by multiplying the GPP and RESP fields with 110/120, 120/120, 130/120, up to 170/120 (7 GPP values around 2007). We then produced time series of these scenarios with increasing productivity (12 GPP increases) by multiplying the GPP and RESP fields following 0.4 to 1.5 times the proportional increase in atmospheric CO_2 (Le Quéré et al., 2018). The resulting 84 GPP and RESP fields still had zero annual sinks or sources at each grid cell. We imprinted on the RESP fields the annual mean carbon sinks of the TRENDY intercomparison project v7 biosphere model ensemble (13 NBP fields, Le Quéré et al., 2018; Sitch et al., 2015). We term the resulting flux variable of releasing CO_2 RECO because it now includes all disturbances present in the TRENDY models such as land use change and fire in addition to respiration fluxes. This gave a full factorial design of plant productivity (7 GPP values around 2007), its increase in time (12 GPP increases), and the annual net land carbon sink (13 NBP fields), where each of the 1,092 scenarios has an a priori good seasonal cycle (from the data) and a realistically annually changing net carbon sink (from the models), while GPP and its increase in time vary over large ranges. The fluxes derived under each scenario were then dispersed spatially in the atmospheric transport model TM3 (Heimann & Körner, 2003) to obtain time-varying atmospheric concentrations. These were evaluated by comparing them against the observed SC at Point Barrow (high latitude, 71°N) and Mauna Loa (low latitude, 20°N). The two stations have the two longest time series of the observational record and provide hence the strongest constraint for the scenarios. Please see the Text S1 in Supporting Information S1 for details.

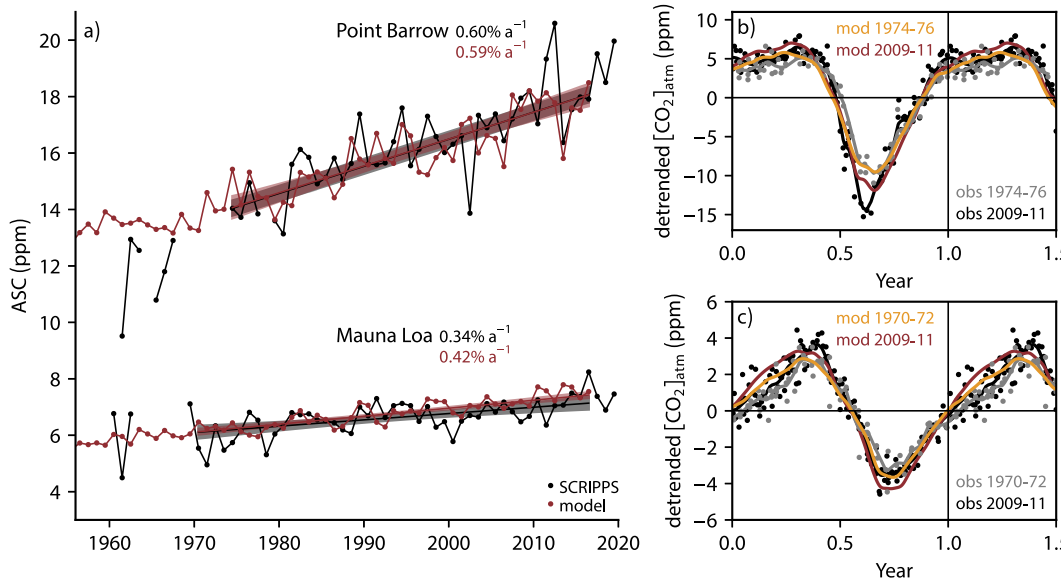

Figure 1. Amplitude of the seasonal cycle and its increase at Point Barrow and Mauna Loa. Observed (SCRIPPS; black) and derived (model; red) seasonal amplitude of atmospheric CO_2 (ASC) at Point Barrow, Alaska (71°N) and Mauna Loa, Hawaii (20°N) (a), as well as seasonal cycles observed and derived at Point Barrow (b) and Mauna Loa (c) for the beginning of the time series at the stations and for the time period from 2009 to 2011 as in Graven et al. (2013). The derived amplitude is the best scenario among a factorial set of scenarios in terms of agreement with the observed ASC. It corresponds to a northern extratropical gross primary productivity (GPP) (>23°N) of 50.5 PgC a^{-1} around 2007, a relative trend of GPP of 1.3 times the relative trend in atmospheric CO_2, and the annual carbon sink distribution from the terrestrial biosphere model ORCHIDEE (Krinner et al., 2005). The shaded areas around the ASC increases in (a) are the 95% confidence intervals of the fitted lines. The increasing ASC trends are given in percentage change per year. In (b) and (c), the first 6 months of the year are repeated.

3. Results and Discussion

We estimated seasonal amplitudes and their trends at Point Barrow and Mauna Loa from daily flask data (Keeling et al., 2005) and found almost identical trends to earlier studies (Graven et al., 2013) of (0.60 ± 0.09)% a^{-1} at Point Barrow and of (0.34 ± 0.12)% a^{-1} at Mauna Loa (Figure 1a), despite different time series lengths and different methods of time series analysis (cf. Text S1 in Supporting Information S1). We found the best combinations of GPP, its trend, and carbon sink distribution by comparing the resulting ASC from the factorial set of scenarios of plant productivity and carbon sinks with the observed ASC at Point Barrow and Mauna Loa. The overall best combination with the lowest RMSE between the trends of ASC has a northern extratropical GPP (>23°N) of 51 PgC a^{-1} around 2007 and a relative trend of GPP of 1.3 times the observed trend in atmospheric CO_2 concentrations, which is an increase of GPP of 0.68% a^{-1} in 2007. It leads to very little bias of the mean ASC of (−0.01 ± 0.01) ppm and (−0.15 ± 0.08) ppm at Point Barrow and Mauna Loa, respectively, and comparable ASC trends of (0.59 ± 0.07)% a^{-1} ($p = 0.96$) and (0.42 ± 0.06)% a^{-1} ($p = 0.52$), respectively. The agreement throughout the whole time series can also be compared visually in Figures 1b and 1c. 32 of the 1,092 scenarios had ASC and increases in accordance with the observations at Point Barrow and Mauna Loa (see Figures S1 and S5 in Supporting Information S1). Their mean northern extratropical GPP was (51 ± 2) PgC a^{-1} around 2007 (corresponding to 151 ± 4 PgC a^{-1} globally) with a mean increase of GPP of (1.1 ± 0.3) times atmospheric CO_2 (Figure 2). The variations given for the mean values are the standard deviation of the 32 scenarios and they should not be seen as formal uncertainties, which would need more formal methods such as Markov Chain Monte-Carlo algorithms (e.g., Andrieu et al., 2003). Contrary to earlier efforts (Haverd et al., 2020; Thomas et al., 2016), it is hence indeed possible to explain ASC and its increase at high and low latitudes when using the correct seasonal dynamics of NBP together with large biospheric productivity (GPP) and a relative increase similar to the increase of atmospheric CO_2. The spatial/latitudinal distribution of the land carbon sink, on the other hand, seems to be of minor importance since the 32 scenarios in accordance with observations include sink estimates from 9 out of the 13 biosphere models, which simulated different latitudinal sink distributions (Figure S3 in Supporting Information S1).

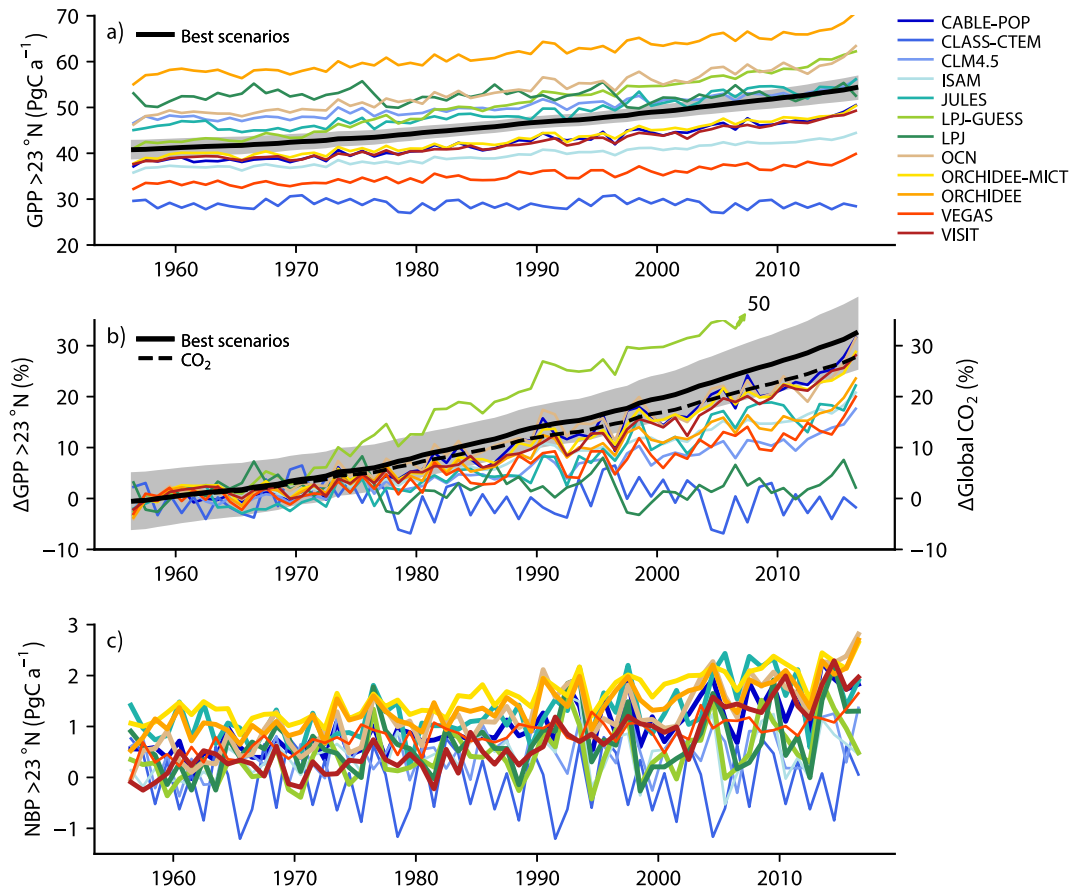

Figure 2. Time series of carbon fluxes of the extratropical northern hemisphere in the TRENDY models. Time series of (a) gross primary productivity (GPP), (b) GPP relative to the mean of the first five years in comparison to the relative increase of atmospheric CO_2, and (c) the annual land sink (net primary productivity, NBP) of the TRENDY v7 models in the extratropical northern hemisphere (>23°N). The thick black lines in (a) and (b) are the mean of the best scenarios (i.e., the 32 scenarios in accordance with the observations at Point Barrow and Mauna Loa, see Figures S1 and S5 in Supporting Information S1) and the shaded areas are the 5- and 95-percentiles of the best scenarios. The dashed line in (b) is the observed global mean CO_2 concentration relative to its mean of the first 5 years. The models that feature in the best scenarios (CABLE-POP, JULES, LPJ, LPJ-GUESS, LPX-Bern, OCN, ORCHIDEE, ORCHIDEE-MICT, and VISIT, cf. Figure S1 in Supporting Information S1) have double the line thickness in (c).

Twenty-six of the 32 scenarios that match ASC and its increase at Point Barrow and at Mauna Loa (i.e., are within the dark gray-shaded target area in Figure S1 in Supporting Information S1; cf. Text S1 in Supporting Information S1) have northern extratropical GPP of 50.5 PgC a^{-1} and large relative trends in GPP of 0.7–1.5 times the relative trend in atmospheric CO_2 (Figure 2). This is within, but at the high end of, the envelope of current estimates from different studies and approaches [see Jung et al. (2020) for a review]. No fitting scenario had GPP values below 47 PgC a^{-1}. Scenarios with large GPP increases but smaller absolute GPP values could give consistent ASC increases only at one of the two sites but not at both, that is, at Point Barrow and Mauna Loa. GPP increases proportionally to CO_2 as an emergent outcome of our analysis, but we make no a priori assumptions about the causes behind GPP increases. CO_2 fertilization increases photosynthesis per unit leaf area, but may also increase leaf area (Haverd et al., 2020) or forest cover (Forkel et al., 2016), which tends to further amplify the GPP increase beyond a proportional change with CO_2 concentration. Cernusak et al. (2019) argued that 1.0 times the relative trend in atmospheric CO_2 should be the maximal response of the terrestrial biosphere to rising CO_2. However, larger relative increases of GPP have been reported based on atmospheric and eddy covariance observations (Chen et al., 2022; Pearman & Hyson, 1981), which includes covariation of increasing CO_2 with other environmental changes such as increasing temperature and growing season length. The increase of ASC, on the other hand, is not sensitive to the strengths of the land carbon sink (Figure 2c) nor its spatial distribution since 9

out of 13 TRENDY v7 models are consistent with ASC and its increase, given northern extratropical GPP is above 47 PgC a^{-1}.

The influential paper of Forkel et al. (2016) mentioned above used the vegetation model LPJmL, which was not part of the model ensemble TRENDY v7 (Sitch et al., 2015), and reported very good ASC trends at Point Barrow and Mauna Loa. It had a global GPP of ca. 148 PgC a^{-1} around 2007 and a relative trend of only 0.5 times the trend in atmospheric CO_2. It showed, however, a bias of about 1 ppm at Mauna Loa (cf. Figure S1 in Supporting Information S1), which is three times larger than our target for Mauna Loa, so that Forkel et al. would not have been considered a suitable scenario in our study.

The scenarios are constructed to have the same seasonal variation of NBP for the whole time period from 1955 to 2016. An earlier growing season, and hence changing seasonal NBP, is often discussed as an essential component of the ASC increase (Keeling et al., 1996; Piao et al., 2008). Randerson et al. (1997, 1999), for example, suggested that NPP must increase especially before June north of 50°N to explain the increase in ASC at high northern latitudes. We argue that this might rather come from a coincidental increase of GPP between model versions used for the simulations that did not fit ASC increases (Randerson et al., 1997) and the simulations that reproduced ASC increases at Point Barrow (Randerson et al., 1999), corresponding to an increase from about 123 to 142 PgC a^{-1} globally around 2007 and hence in alignment with our study. Other studies have also shown that an earlier growing season is not sufficient to explain the observed increase of ASC (Piao et al., 2008; Thomas et al., 2016). We show here that an earlier growing season is not necessary to explain ASC and its increases at mid and high northern latitudes. It does not mean that an earlier growing season does not yield more productivity. We argue that an earlier growing season might lead to an earlier sink but it might not change the timing of the maximum drawdown (maximum NBP). However, this could be verified with long-term flux observations at high northern latitudes (Virkkala et al., 2021).

The 32 scenarios that match ASC and its increase concentrate consistently around northern extratropical GPP of (51 ± 2) PgC a^{-1} around 2007, with corresponding global GPP values of (151 ± 4) PgC a^{-1}. The TRENDY v7 models simulate a large spread of global GPP values from 97 to 204 PgC a^{-1} around 2007 (mean 140 PgC a^{-1}) with only two models close to 150 PgC a^{-1} (Figure S2a in Supporting Information S1). However, temperate and boreal/arctic ecosystems (>23°N) shape ASC in the northern hemisphere (Lin et al., 2020). This is also true in our analysis, which was insensitive to productivity changes in the tropics. About half of the TRENDY models are within 15% of the best scenarios for northern extratropical GPP, at least at the end of the time series (Figure 2a), so that such a high northern hemispheric productivity seems consistent with bottom-up estimates of the fluxes by those models. Our analysis cannot differentiate between different sink regions within the northern extratropics. Lin et al. (2020), however, found with tagged model experiments that the ASC increase is dominated by Siberian and temperate regions while arctic-boreal North America and Europe play almost no role. Liu et al. (2024) argued that climatic and environmental characteristics differ notably between Eurasian and North American boreal forests and that satellite-derived increases of LAI have been more persistent in Eurasia than North America (Berner & Goetz, 2022; Xu et al., 2013). However, this is not corroborated by independent, satellite-based estimates of GPP increases from solar-induced chlorophyll fluorescence, which show very similar and persistent increases of GPP in both Eurasia and North America (Li & Xiao, 2019).

Only two TRENDY models exhibit a relative trend close to 1.0 times the observed trend in CO_2 on the global scale (CABLE-POP and LPJ-GUESS, Figure S2 in Supporting Information S1), while four models estimate such a large trend in the northern extratropics, where LPJ-GUESS simulates a trend as high as 1.7 times that of atmospheric CO_2 (Figure 2). It was, however, not possible to reproduce the observed ASC using the fluxes from the TRENDY models directly as the seasonal variations of GPP and RECO in the models are inconsistent with the data (Haverd et al., 2020). It is the combination of the seasonal variations from the data-driven products and annual carbon sink estimates from the TRENDY v7 models—as the only information used from those models in our analysis—that allowed our study to match the observed ASC.

Note that northern extratropical RECO is also confined to (50 ± 3) PgC a^{-1} around 2007 in our study, with the difference to GPP being the land carbon sink. RECO follows the same trend of GPP here and RECO can hence be discussed only marginally in our analysis. It was however used to estimate GPP on the global scale, using the same source-driven approach than our study (Jian et al., 2022).

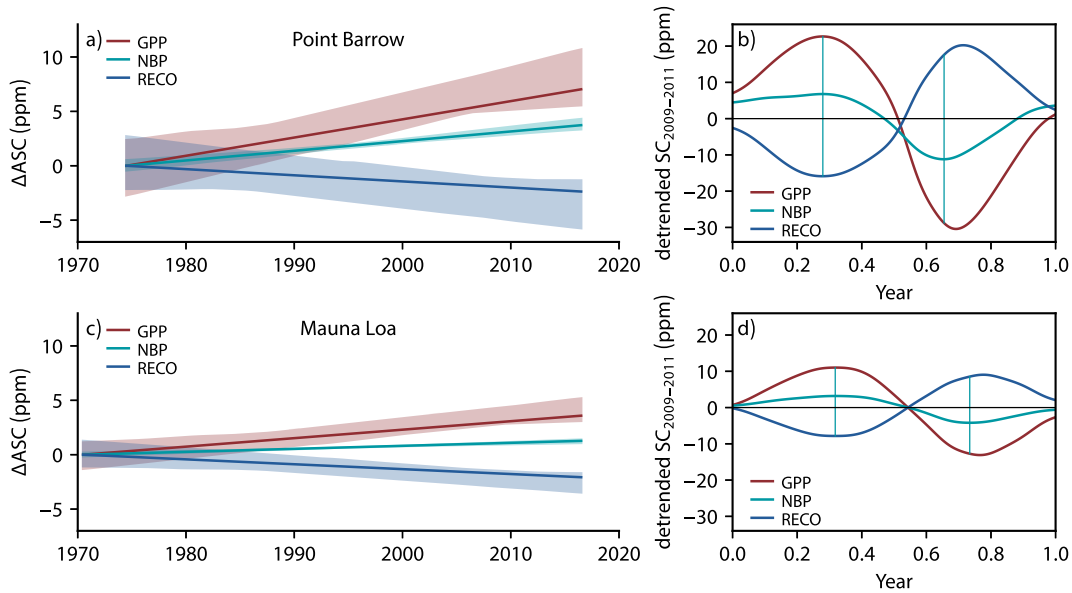

Figure 3. Contribution of photosynthesis and respiration to the increase of the seasonal amplitude for the best scenarios. Contribution of photosynthesis (gross primary productivity (GPP), red) and respiration (RECO, blue) to the derived increase of ASC (NBP, green) at Point Barrow (a) and Mauna Loa (c) of the best scenarios. The shaded areas are the 5- and 95-percentiles and the solid lines are the mean contributions of the best scenarios. Seasonal Cycles of photosynthesis (GPP, red) and respiration (RECO, blue) of the overall best scenario transported in the atmosphere with TM3, and of the combined signal (NBP, green), which is the derived ASC at Point Barrow (b) and Mauna Loa (d) for the time period from 2009 to 2011. The vertical green lines indicate the times of the maximum and minimum NBP (green) at which the contributions of GPP and RECO are calculated.

We quantified the contributions of photosynthesis (GPP) and respiration (RECO) to the increase of ASC in the 32 best scenarios that match ASC and its increase at Point Barrow and Mauna Loa by transporting GPP and RECO independently in the tracer transport model TM3. The contribution of GPP (RECO) is the difference of the detrended smooth curve of GPP (RECO) at the maximum and minimum of the NBP seasonal cycle (see Materials and Methods and Figure 3b). This is different to other estimates of the contributions of GPP and RECO to the increase of ASC. Forkel et al. (2016) used the increases of GPP and RECO as a proxy for their contributions to increasing ASC. But the increase of GPP must be greater than the increase of RECO if the annual net sink, NBP = GPP—RECO, increases as well, which gives hence the contributions of GPP and RECO to the atmospheric growth rate but not to the seasonal cycle. Bacastow et al. (1985) and Liu et al. (2024) used the trends in the maxima and minima of ASC as a proxy for the contributions of GPP and RECO to ASC increases. The two signals are, however, not independent information and also depend strongly on the chosen method to remove the long-term trend in the CO_2 concentrations, as pointed out by Bacastow et al. (1985). We argue that using directly the transported atmospheric signals of GPP and RECO most accurately reveals the contributions of GPP and RECO to increasing ASC. Figure 3a shows the contributions relative to the start of the analysis. We found that GPP has by far the largest contribution to ASC increase, while RECO counteracts the increase of GPP at Point Barrow and Mauna Loa. This is consistent with observations that seasonal variations of NEE are strongly related to absolute GPP fluxes in the northern extratropics (Beer et al., 2010).

RECO counteracts the large ASC from GPP. This counterbalance can change with increasing fluxes or with changing seasonality of the fluxes. The relative contributions of GPP and RECO might hence be underrepresented in our approach because it does not include a lengthening of the growing season (Keeling et al., 1996) nor enhanced respiration due to warmer autumn temperatures in Eurasia (Piao et al., 2008). As argued above, a changing growing season might lead to earlier sinks and varying autumn respiration (Barichivich et al., 2013) but it does most probably not change the timing of the maxima of the fluxes GPP and RECO, respectively. We hence believe that our analysis shows a robust signal of a dominant contribution of GPP to increasing ASC. It would be possible to construct source/sink scenarios that include a lengthening of the growing season but the corresponding uncertainties would be large and would most probably not lead to conclusive results. Long-term flux observations

at high northern latitudes could potentially reduce the uncertainties but current estimates of fluxes in the boreal and tundra regions still largely diverge (Jung et al., 2011; Nelson et al., 2024; Virkkala et al., 2021).

4. Conclusions

We reveal a productive terrestrial biosphere in the northern hemisphere that was highly stimulated by rising CO_2 concentrations and concomitant environmental changes during the last 40 years. Variations among the scenarios that matched the observed ASC and its increase over time were small and thus provide robust evidence for our finding of large plant productivity of northern ecosystems, with a large increase that is about proportional to the increase in atmospheric CO_2. The constraint we have identified demonstrates that current terrestrial biosphere models, collectively, are unable to reproduce *both* the ASC *and* its increase (Haverd et al., 2020; Thomas et al., 2016), signaling biases in the models. It is worthwhile to work on the timing of the individual fluxes GPP and RECO in the biosphere models, but also in data-based estimates, so that the increase in ASC can be used as an additional, previously unavailable, independent, and robust constraint of absolute GPP.

Data Availability Statement

Gross primary productivity and net ecosystem exchange from Jung et al. (2011) can freely be downloaded from the Data Exchange Portal of the Max Planck Institute of Biogeochemistry, Jena, Germany (www.bgc-jena.mpg.de/geodb/). To access the data, choose the project BGI after accepting the data usage agreement. The version used in this manuscript was acquired from the iLAMB project (https://github.com/rubisco-sfa/ILAMB-Data/). Net carbon sinks from the TRENDY v7 terrestrial biosphere models were provided by the Global Carbon Project (www.globalcarbonproject.org), are stored at and can freely be downloaded from the Global Carbon Budget Data following the links provided at https://globalcarbonbudgetdata.org/closed-access-requests.html. Access to versions before TRENDY v10 are provided on demand by Mike O'Sullivan of the University of Exeter, UK. Model code of the atmospheric transport model TM3 can be obtained by contacting Christian Rödenbeck of the Max Planck Institute for Biogeochemistry, Jena, Germany. He also provides model forcing files using NCEP reanalysis data from NOAA's Physical Sciences Laboratory (https://psl.noaa.gov/).

Acknowledgments

High Performance Computing resources have been provided by the National Computational Infrastructure (NCI Australia), an NCRIS enabled capability supported by the Australian Government, and the center EXPLOR, hosted by the University of Lorraine (project 2018A2FXX0454). M.C. acknowledges support from a CSIRO Frohlich fellowship, a French National Research Agency (ANR) grant ANR-21-CE02-0033-01, and a grant overseen by ANR as part of the "Investissements d'Avenir" program (ANR-11-LABX-0002-01, Lab of Excellence ARBRE). V.H. and J.G.C. acknowledge support from Australia's National Environmental Science Program —Climate Systems Hub. We thank Sara Mikaloff-Fletcher (NIWA Wellington, New Zealand) for the provision of the TM3 transport code and Christian Rödenbeck (MPI-BGC Jena, Germany) for provision of the NCEP-based forcing fields. We thank the TRENDY team for the provision of the DGVM simulations, and the researchers of the Global Carbon Project for making their data publicly available.

References

Andrieu, C., de Freitas, N., Doucet, A., & Jordan, M. I. (2003). An introduction to MCMC for machine learning. *Machine Learning*, *50*(1), 5–43. https://doi.org/10.1023/A:1020281327116

Bacastow, R. B., Keeling, C. D., & Whorf, T. P. (1985). Seasonal amplitude increase in atmospheric CO_2 concentration at Mauna Loa, Hawaii, 1959–1982. *Journal of Geophysical Research*, *90*(D6), 10529–10540. https://doi.org/10.1029/JD090iD06p10529

Barichivich, J., Briffa, K. R., Myneni, R. B., Osborn, T. J., Melvin, T. M., Ciais, P., et al. (2013). Large-scale variations in the vegetation growing season and annual cycle of atmospheric CO_2 at high northern latitudes from 1950 to 2011. *Global Change Biology*, *19*(10), 3167–3183. https://doi.org/10.1111/gcb.12283

Beer, C., Reichstein, M., Tomelleri, E., Ciais, P., Jung, M., Carvalhais, N., et al. (2010). Terrestrial gross carbon dioxide uptake: Global distribution and covariation with climate. *Science*, *329*(5993), 834–838. https://doi.org/10.1126/science.1184984

Berner, L. T., & Goetz, S. J. (2022). Satellite observations document trends consistent with a boreal forest biome shift. *Global Change Biology*, *28*(10), 3275–3292. https://doi.org/10.1111/gcb.16121

Buermann, W., Lintner, B. R., Koven, C. D., Angert, A., Pinzon, J. E., Tucker, C. J., & Fung, I. Y. (2007). The changing carbon cycle at Mauna Loa Observatory. *Proceedings of the National Academy of Sciences*, *104*(11), 4249–4254. https://doi.org/10.1073/pnas.0611224104

Cernusak, L. A., Haverd, V., Brendel, O., Le Thiec, D., Guehl, J.-M., & Cuntz, M. (2019). Robust response of terrestrial plants to rising CO_2. *Trends in Plant Science*, *24*(7), 578–586. https://doi.org/10.1016/j.tplants.2019.04.003

Chen, C., Park, T., Wang, X., Piao, S., Xu, B., Chaturvedi, R. K., et al. (2019). China and India lead in greening of the world through land-use management. *Nature Sustainability*, *2*(2), 122–129. https://doi.org/10.1038/s41893-019-0220-7

Chen, C., Riley, W. J., Prentice, I. C., & Keenan, T. F. (2022). CO_2 fertilization of terrestrial photosynthesis inferred from site to global scales. *Proceedings of the National Academy of Sciences*, *119*(10), e2115627119. https://doi.org/10.1073/pnas.2115627119

Collier, N., Hoffman, F. M., Lawrence, D. M., Keppel-Aleks, G., Koven, C. D., Riley, W. J., et al. (2018). The international land model benchmarking (ILAMB) system: Design, theory, and implementation. *Journal of Advances in Modeling Earth Systems*, *10*(11), 2731–2754. https://doi.org/10.1029/2018MS001354

Cuntz, M., Ciais, P., Hoffmann, G., Allison, C. E., Francey, R., Knorr, W., et al. (2003). A comprehensive global three-dimensional model of $\delta^{18}O$ in atmospheric CO_2: 2. Mapping the atmospheric signal. *Journal of Geophysical Research*, *108*(D17), 4528. https://doi.org/10.1029/2002JD003154

Efron, B. (1981). Nonparametric estimates of standard error - The jackknife, the bootstrap and other methods. *Biometrika*, *68*(3), 589–599. https://doi.org/10.2307/2335441

Forkel, M., Carvalhais, N., Rödenbeck, C., Keeling, R., Heimann, M., Thonicke, K., et al. (2016). Enhanced seasonal CO_2 exchange caused by amplified plant productivity in northern ecosystems. *Science*, *351*(6274), 696–699. https://doi.org/10.1126/science.aac4971

Graven, H. D., Keeling, R. F., Piper, S. C., Patra, P. K., Stephens, B. B., Wofsy, S. C., et al. (2013). Enhanced seasonal exchange of CO_2 by northern ecosystems since 1960. *Science*, *341*(6150), 1085–1089. https://doi.org/10.1126/science.1239207

Gray, J. M., Frolking, S., Kort, E. A., Ray, D. K., Kucharik, C. J., Ramankutty, N., & Friedl, M. A. (2014). Direct human influence on atmospheric CO_2 seasonality from increased cropland productivity. *Nature*, *515*(7527), 398–401. https://doi.org/10.1038/nature13957

Gurney, K. R., Law, R. M., Denning, A. S., Rayner, P. J., Pak, B. C., Baker, D., et al. (2004). Transcom 3 inversion intercomparison: Model mean results for the estimation of seasonal carbon sources and sinks. *Global Biogeochemical Cycles*, *18*(1), GB1010. https://doi.org/10.1029/2003GB002111

Härdle, W., & Müller, M. (2000). Multivariate and semiparametric kernel regression. In M. G. Schimek (Ed.), *Smoothing and regression: Approaches, computation, and application* (pp. 357–391). John Wiley and Sons, Inc. https://doi.org/10.1002/9781118150658.ch12

Haverd, V., Smith, B., Canadell, J. G., Cuntz, M., Mikaloff Fletcher, S., Farquhar, G., et al. (2020). Higher than expected CO_2 fertilization inferred from leaf to global observations. *Global Change Biology*, *26*(4), 2390–2402. https://doi.org/10.1111/gcb.14950

Heimann, M., & Körner, S. (2003). *The global atmospheric tracer model TM3*. (Technical Reports—Max Planck Institute for Biogeochemistry 5, p. 131).

Ito, A., Inatomi, M., Huntzinger, D. N., Schwalm, C., Michalak, A. M., Cook, R., et al. (2016). Decadal trends in the seasonal-cycle amplitude of terrestrial CO_2 exchange resulting from the ensemble of terrestrial biosphere models. *Tellus Series B*, *68*(1), 28968. https://doi.org/10.3402/tellusb.v68.28968

Jian, J., Bailey, V., Dorheim, K., Konings, A. G., Hao, D., Shiklomanov, A. N., et al. (2022). Historically inconsistent productivity and respiration fluxes in the global terrestrial carbon cycle. *Nature Communications*, *13*(1), 1733. https://doi.org/10.1038/s41467-022-29391-5

Jung, M., Reichstein, M., Margolis, H. A., Cescatti, A., Richardson, A. D., Arain, M. A., et al. (2011). Global patterns of land-atmosphere fluxes of carbon dioxide, latent heat, and sensible heat derived from eddy covariance, satellite, and meteorological observations. *Journal of Geophysical Research*, *116*(G00J07), 16. https://doi.org/10.1029/2010JG001566

Jung, M., Schwalm, C., Migliavacca, M., Walther, S., Camps-Valls, G., Koirala, S., et al. (2020). Scaling carbon fluxes from eddy covariance sites to globe: Synthesis and evaluation of the FLUXCOM approach. *Biogeosciences*, *17*(5), 1343–1365. https://doi.org/10.5194/bg-17-1343-2020

Kalnay, E., Kanamitsu, M., Kistler, R., Collins, W., Deaven, D., Gandin, L., et al. (1996). The NCEP/NCAR 40-Year reanalysis project. *Bulletin of the American Meteorological Society*, *77*(3), 437–472. https://doi.org/10.1175/1520-0477(1996)077<0437:TNYRP>2.0.CO;2

Keeling, C. D., Chin, J. F. S., & Whorf, T. P. (1996). Increased activity of northern vegetation inferred from atmospheric CO_2 measurements. *Nature*, *382*(6587), 146–149. https://doi.org/10.1038/382146a0

Keeling, C. D., Piper, S. C., Bacastow, R. B., Wahlen, M., Whorf, T. P., Heimann, M., & Meijer, H. A. (2005). Atmospheric CO_2 and $^{13}CO_2$ exchange with the terrestrial biosphere and oceans from 1978 to 2000: Observations and carbon cycle implications. In I. T. Baldwin, M. M. Caldwell, G. Heldmaier, R. B. Jackson, O. L. Lange, H. A. Mooney, et al. (Eds.), *A history of atmospheric CO_2 and its effects on plants, animals, and ecosystems* (pp. 83–113). Springer New York. https://doi.org/10.1007/0-387-27048-5_5

Krinner, G., Viovy, N., de Noblet-Ducoudre, N., Ogée, J., Polcher, J., Friedlingstein, P., et al. (2005). A dynamic global vegetation model for studies of the coupled atmosphere-biosphere system. *Global Biogeochemical Cycles*, *19*(1), GB1015. https://doi.org/10.1029/2003GB002199

Le Quéré, C., Andrew, R. M., Friedlingstein, P., Sitch, S., Pongratz, J., Manning, A. C., et al. (2018). Global carbon budget 2017. *Earth System Science Data*, *10*(1), 405–448. https://doi.org/10.5194/essd-10-405-2018

Li, X., & Xiao, J. (2019). Mapping photosynthesis solely from solar-induced chlorophyll fluorescence: A global, fine-resolution dataset of gross primary production derived from OCO-2. *Remote Sensing*, *11*(21), 2563. https://doi.org/10.3390/rs11212563

Lin, X., Rogers, B. M., Sweeney, C., Chevallier, F., Arshinov, M., Dlugokencky, E., et al. (2020). Siberian and temperate ecosystems shape Northern Hemisphere atmospheric CO_2 seasonal amplification. *Proceedings of the National Academy of Sciences USA*, *117*(35), 21079–21087. https://doi.org/10.1073/pnas.1914135117

Liu, Z., Rogers, B. M., Keppel-Aleks, G., Helbig, M., Ballantyne, A. P., Kimball, J. S., et al. (2024). Seasonal CO_2 amplitude in northern high latitudes. *Nature Reviews Earth and Environment*, *5*(11), 802–817. https://doi.org/10.1038/s43017-024-00600-7

Nelson, J. A., Walther, S., Gans, F., Kraft, B., Weber, U., Novick, K., et al. (2024). X-BASE: The first terrestrial carbon and water flux products from an extended data-driven scaling framework, FLUXCOM-X. *Biogeosciences*, *21*(22), 5079–5115. https://doi.org/10.5194/bg-21-5079-2024

Pearman, G. I., & Hyson, P. (1981). The annual variation of atmospheric CO_2 concentration observed in the northern hemisphere. *Journal of Geophysical Research*, *86*(C10), 9839–9843. https://doi.org/10.1029/JC086iC10p09839

Peng, S., Ciais, P., Chevallier, F., Peylin, P., Cadule, P., Sitch, S., et al. (2015). Benchmarking the seasonal cycle of CO_2 fluxes simulated by terrestrial ecosystem models. *Global Biogeochemical Cycles*, *29*(1), 46–64. https://doi.org/10.1002/2014GB004931

Piao, S., Ciais, P., Friedlingstein, P., Peylin, P., Reichstein, M., Luyssaert, S., et al. (2008). Net carbon dioxide losses of northern ecosystems in response to autumn warming. *Nature*, *451*(7174), 49–52. https://doi.org/10.1038/nature06444

Piao, S., Liu, Z., Wang, Y., Ciais, P., Yao, Y., Peng, S., et al. (2017). On the causes of trends in the seasonal amplitude of atmospheric CO_2. *Global Change Biology*, *24*(2), 608–616. https://doi.org/10.1111/gcb.13909

Randerson, J. T., Field, C. B., Fung, I. Y., & Tans, P. P. (1999). Increases in early season ecosystem uptake explain recent changes in the seasonal cycle of atmospheric CO_2 at high northern latitudes. *Geophysical Research Letters*, *26*(17), 2765–2768. https://doi.org/10.1029/1999GL900500

Randerson, J. T., Thompson, M. V., Conway, T. J., Fung, I. Y., & Field, C. B. (1997). The contribution of terrestrial sources and sinks to trends in the seasonal cycle of atmospheric carbon dioxide. *Global Biogeochemical Cycles*, *11*(4), 535–560. https://doi.org/10.1029/97GB02268

Schulzweida, U. (2022). *CDO user guide*. Zenodo. https://doi.org/10.5281/zenodo.1435454

Sitch, S., Friedlingstein, P., Gruber, N., Jones, S. D., Murray-Tortarolo, G., Ahlström, A., et al. (2015). Recent trends and drivers of regional sources and sinks of carbon dioxide. *Biogeosciences*, *12*(3), 653–679. https://doi.org/10.5194/bg-12-653-2015

Thomas, R. T., Prentice, I. C., Graven, H., Ciais, P., Fisher, J. B., Hayes, D. J., et al. (2016). Increased light-use efficiency in northern terrestrial ecosystems indicated by CO_2 and greening observations. *Geophysical Research Letters*, *43*(21), 11339–11349. https://doi.org/10.1002/2016GL070710

Thoning, K. W., Tans, P. P., & Komhyr, W. D. (1989). Atmospheric carbon dioxide at Mauna Loa observatory: 2. Analysis of the NOAA GMCC data, 1974–1985. *Journal of Geophysical Research*, *94*(6), 8549–8565. https://doi.org/10.1029/jd094id06p08549

Virkkala, A., Aalto, J., Rogers, B. M., Tagesson, T., Treat, C. C., Natali, S. M., et al. (2021). Statistical upscaling of ecosystem CO_2 fluxes across the terrestrial tundra and boreal domain: Regional patterns and uncertainties. *Global Change Biology*, *27*(17), 4040–4059. https://doi.org/10.1111/gcb.15659

Wang, K., Wang, Y., Wang, X., He, Y., Li, X., Keeling, R. F., et al. (2020). Causes of slowing-down seasonal CO_2 amplitude at Mauna Loa. *Global Change Biology*, *26*(8), 4462–4477. https://doi.org/10.1111/gcb.15162

Xu, L., Myneni, R. B., Chapin III, F. S., Callaghan, T. V., Pinzon, J. E., Tucker, C. J., et al. (2013). Temperature and vegetation seasonality diminishment over northern lands. *Nature Climate Change*, *3*(6), 581–586. https://doi.org/10.1038/nclimate1836

Yun, J., Jeong, S., Gruber, N., Gregor, L., Ho, C.-H., Piao, S., et al. (2022). Enhance seasonal amplitude of atmospheric CO_2 by the changing Southern Ocean carbon sink. *Science Advances*, *8*(41), eabq0220. https://doi.org/10.1126/sciadv.abq0220

Zeng, N., Zhao, F., Collatz, G. J., Kalnay, E., Salawitch, R. J., West, T. O., & Guanter, L. (2014). Agricultural Green Revolution as a driver of increasing atmospheric CO_2 seasonal amplitude. *Nature*, *515*(7527), 394–397. https://doi.org/10.1038/nature13893

Zhu, Z., Piao, S., Yan, T., Ciais, P., Bastos, A., Zhang, X., & Wang, Z. (2018). The accelerating land carbon sink of the 2000s may not be driven predominantly by the warming hiatus. *Geophysical Research Letters*, *45*(3), 1402–1409. https://doi.org/10.1002/2017GL075808